

Exceptional Chemotherapy Response in Metastatic Colorectal Cancer Associated With Hyper-Indel–Hypermuted Cancer Genome and Comutation of *POLD1* and *MLH1*

Manish R. Sharma

James T. Auman

Nirali M. Patel

Juneko E. Grilley-Olson

Xiaobei Zhao

Stergios J. Moschos

Joel S. Parker

Xiaoying Yin

Michele C. Hayward

Blase N. Polite

Elena Marangon

Bianca Posocco

Giuseppe Toffoli

D. Neil Hayes

Federico Innocenti

Author affiliations and support information appear at the end of this article.

M.R.S. and J.T.A. contributed equally to this work.

The content is solely the responsibility of the authors and does not necessarily represent the official views of the National Cancer Institute or National Institutes of Health.

Corresponding author: D. Neil Hayes, MD, Lineberger Comprehensive Cancer Center, University of North Carolina at Chapel Hill, CB #7295, 125 Mason Farm Road, Chapel Hill, NC 27599; e-mail: hayes@med.unc.edu.

abstract

Purpose A 73-year-old woman with metastatic colon cancer experienced a complete response to chemotherapy with dose-intensified irinotecan that has been durable for 5 years. We sequenced her tumor and germ line DNA and looked for similar patterns in publicly available genomic data from patients with colorectal cancer.

Patients and Methods Tumor DNA was obtained from a biopsy before therapy, and germ line DNA was obtained from blood. Tumor and germline DNA were sequenced using a commercial panel with approximately 250 genes. Whole-genome amplification and exome sequencing were performed for *POLE* and *POLD1*. A *POLD1* mutation was confirmed by Sanger sequencing. The somatic mutation and clinical annotation data files from the colon (n = 461) and rectal (n = 171) adenocarcinoma data sets were downloaded from The Cancer Genome Atlas data portal and analyzed for patterns of mutations and clinical outcomes in patients with *POLE*- and/or *POLD1*-mutated tumors.

Results The pattern of alterations included *APC* biallelic inactivation and microsatellite instability high (MSI-H) phenotype, with somatic inactivation of *MLH1* and hypermutation (estimated mutation rate > 200 per megabase). The extremely high mutation rate led us to investigate additional mechanisms for hypermutation, including loss of function of *POLE*. *POLE* was unaltered, but a related gene not typically associated with somatic mutation in colon cancer, *POLD1*, had a somatic mutation c.2171G>A [p.Gly724Glu]. Additionally, we noted that the high mutation rate was largely composed of dinucleotide deletions. A similar pattern of hypermutation (dinucleotide deletions, *POLD1* mutations, MSI-H) was found in tumors from The Cancer Genome Atlas.

Conclusion *POLD1* mutation with associated MSI-H and hyper-indel–hypermuted cancer genome characterizes a previously unrecognized variant of colon cancer that was found in this patient with an exceptional response to chemotherapy.

INTRODUCTION

A 73-year-old white woman presented with abdominal pain, fatigue, and weight loss. Her hemoglobin was 7 g/dL. Colonoscopy showed a cecal mass, and biopsy showed invasive adenocarcinoma. She had blood transfusions, with an appropriate increase in her hemoglobin. Her medical history

was significant for back surgery, depression, diverticulitis, hyperlipidemia, hypothyroidism, and osteoporosis. Medications received were alendronate, escitalopram, levothyroxine, and rosuvastatin. Family history was significant for a daughter having had acute lymphoblastic leukemia as a child and her mother having died as a result of breast cancer at age

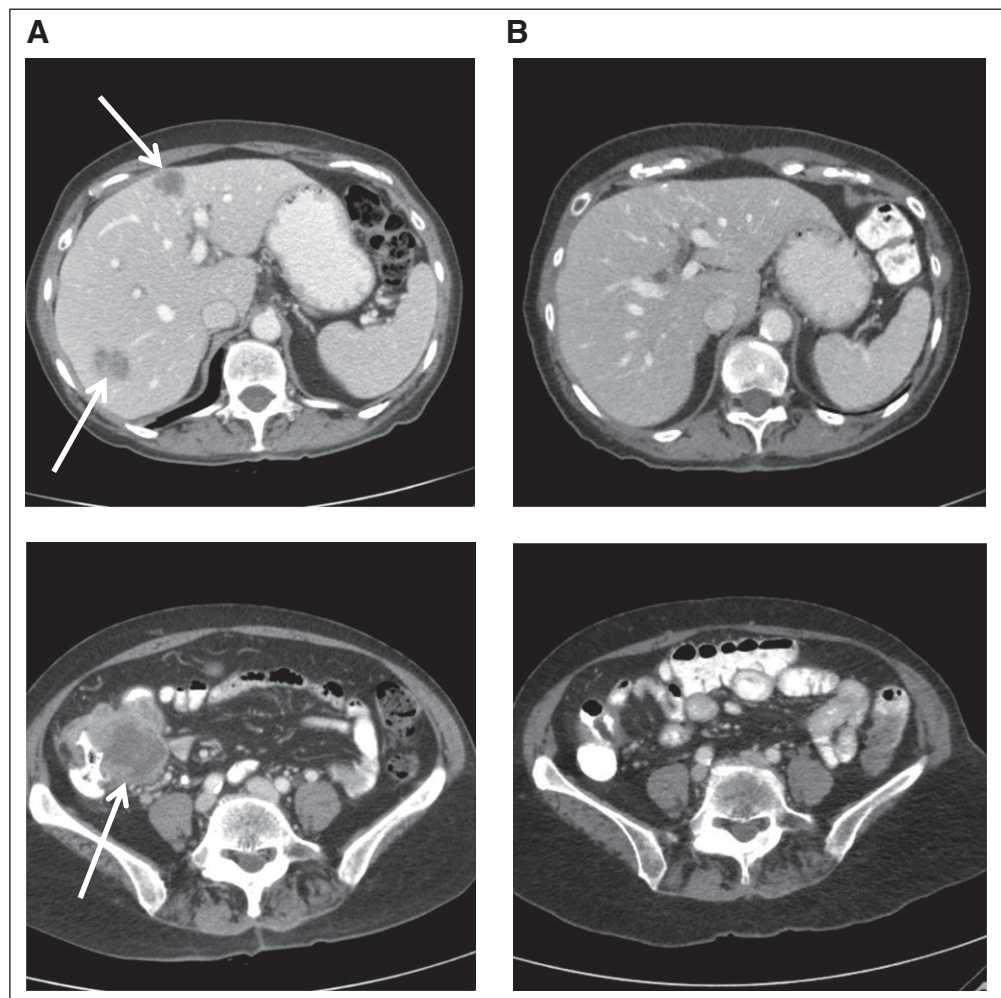
63 years. She was a never-smoker and drank alcohol occasionally. On physical examination, she was well appearing and without any palpable lymphadenopathy, mass, or hepatosplenomegaly. Laboratory findings were notable for hemoglobin 11.2 g/dL (mean corpuscular volume, 75 fL), carcinoembryonic antigen 2.2 ng/mL (reference range, 0 to 3.4 ng/mL), and total bilirubin 0.3 mg/dL. Computed tomography (CT; Fig 1) showed diffuse lymphadenopathy (para-aortic lymph node, 2.6×1.6 cm; portocaval lymph node, 3.1×2.9 cm), bilobar liver metastases (segment 4B lesion, 1.9×1.8 cm; segment 6 lesion, 2.1×2.6 cm), and a cecal mass measuring 4.8×6 cm.

She enrolled in a genotype-guided dosing study of FOLFIRI (fluorouracil [FU], leucovorin, and irinotecan) plus bevacizumab (ClinicalTrials.gov identifier NCT01183494). The objective of this study was to define the maximum-tolerated dose of irinotecan in FOLFIRI plus bevacizumab as first-line therapy in metastatic colorectal cancer, with dosing of irinotecan based on *UGT1A1* genotype.¹

Her *UGT1A1* genotype was $*1/*28$, and she was assigned to receive irinotecan at a dose of 310 mg/m^2 intravenously (IV), 72% higher than the standard dose of 180 mg/m^2 . She received standard doses of the other drugs: FU 400 mg/m^2 IV bolus, then $2,400 \text{ mg/m}^2$ IV over 46 hours; leucovorin 200 mg/m^2 IV; and bevacizumab 5 mg/kg IV. After her first dose, she was hospitalized with grade 3 neutropenia and grade 3 diarrhea. Her second dose was delayed 1 week, and the irinotecan dose was reduced to 233 mg/m^2 . She continued to receive chemotherapy once every 2 weeks with no additional grade 3 adverse events.

She experienced a complete response (CR) to chemotherapy. CT after four doses showed a partial response by RECIST,² with a 44% reduction in target lesions. She had additional reductions after eight and 12 doses. After 14 doses, she elected to discontinue treatment and continued to undergo surveillance CT scans (initially once every 3 months). Eventually, the liver lesions were no longer visible, and all lymph nodes were smaller

Fig 1. Selected images from (A) baseline (pretreatment, 2010) and (B) most recent (post-treatment, 2015) computed tomography scans for this patient. Arrows indicate liver metastases (upper image) and primary tumor in the cecum (lower image).



than 1 cm in short-axis dimension. Her most recent CT, 53 months after discontinuing therapy, showed no evidence of disease (Fig 1), and her CEA has remained within normal limits. A colonoscopy was attempted 29 months after discontinuing therapy but was incomplete because of severe diverticulosis in the sigmoid colon that caused narrowing and looping of the scope. Clinically, she is doing well and is active. On the basis of her durable CR to chemotherapy, she was able to enter a clinical protocol to characterize the molecular alterations of her cancer.

PATIENTS AND METHODS

Tumor from the colonoscopic biopsy and a comparative normal sample (a single acid citrate dextrose tube of blood) were obtained and analyzed according to procedures outlined in the University of North Carolina (UNC) Institutional Review Board–approved protocol (ClinicalTrials.gov identifier NCT01457196; UNCseq LCCC1108), and clinical data were obtained according to Health Insurance Portability and Accountability Act standards. DNA from tumor and normal samples were processed through the usual LCCC1108 production pipeline of targeted capture sequencing as described previously, with a modification for small-volume input of less than 1 μ g of input tumor DNA.³ Briefly, tumor and normal samples were sequenced using commercial protocols (Agilent SureSelect custom targeted panel of approximately 250 genes; Santa Clara, CA) and the Illumina HiSeq platform (San Diego, CA) in either single- or paired-end format of 75 and 100 bases per end. Average depth of coverage for target sequences was 665 reads in the tumor sample and 293 reads in the germline sample. Raw sequencing images were converted to FASTQ file format using Illumina CASAVA software (version 1.8.2; http://support.illumina.com/sequencing/sequencing_software/casava.html). The sequence reads were aligned to the genome using the bwa mem algorithm (version 0.7.4; <https://sourceforge.net/projects/bio-bwa/>) with the default parameters. Realignment was performed simultaneously for tumor and normal pairs using ABRA (version 0.46; <https://github.com/mozack/abra>) with the default parameters. Variants were called using FreeBayes (<https://github.com/ekg/freebayes>) and somatic mutations using Strelka (<http://strelka@ftp.illumina.com/>). Copy number assessments were performed using custom software. Quality statistics were generated with Picard (<https://broadinstitute.github.io/picard/>) and included measures of fragment length, sequence content, alignment, capture bias and efficiency,

coverage, and variant call metrics. Final somatic calls were filtered to require a Strelka-assigned quality of at least 30. All variants were annotated in their gene-specific context using SnpEff (version 3.1; <http://snpeff.sourceforge.net/download.html>) and crossed with COSMIC and internal databases that captured the information from the UNC Clinical Committee for Genomic Research.³

To search for additional mutations in *POLE* and *POLD1*, remaining tumor DNA was subjected to whole-genome amplification using the REPLI-g FFPE kit (QIAGEN Science, Germantown, PA) according to the manufacturer's technical notes for low-input tumor. Whole-exome sequencing was performed, and the identical informatics pipeline was applied.

Focal validation of the *POLD1* mutation was performed on the whole-genome–amplified DNA using Sanger sequencing. Primers were designed to flank exons 18 and 26 of *POLD1* and exon 6 of *POLE*: *POLD1* exon 18: 5'-GCATGATTCTCTC-CCCGACAG-3' (forward) and 5'-CTGCCCTGGCCCATCTCA-3' (reverse); *POLD1* exon 26: 5'-CCGGGAGTCTGAGCTGTATC-3' (forward) and 5'-CAGGGTTCGGGACATGGCA-3' (reverse); and *POLE* exon 6: 5'-CTCTTGAACCA-ATGAGCGTGA-3' (forward) and 5'-GTCGTTCTGAACCGCTGATG-3' (reverse). Polymerase chain reaction amplification and Sanger sequencing were performed using a previously validated protocol within the UNC Hospitals Molecular Genetics Laboratory (Chapel Hill, NC).

The somatic mutation and clinical annotation data files from the colon (n = 461) and rectal (n = 171) adenocarcinoma data sets were downloaded from The Cancer Genome Atlas (TCGA) data portal.⁴ Of these 632 patient cases, 430 (colon, n = 330; rectum, n = 99; unknown, n = 1) contained both somatic mutation and clinical annotation data points. The demographic and clinical characteristics of the 430 patient cases are summarized in Appendix Table A1. For each patient case, the nonsilent somatic mutations and indels were determined from the combined colorectal somatic mutation file. Statistical tests between groups were performed using two-sided *t* test.

RESULTS

Hybrid-Based Targeted Capture Sequencing and Analysis

A colonoscopic biopsy (2.1 \times 0.3 \times 0.3 cm in aggregate) provided the only tumor tissue available. A hematoxylin and eosin section was made from the residual tumor block (Fig 2), and the

remainder was entirely sectioned for the purpose of obtaining DNA. The tumor was confirmed to be a moderately differentiated adenocarcinoma by study pathologists, and the percentage of tumor nuclei was estimated at 60%. The sequencing quality was acceptable for analysis per protocol standards as characterized by inspection library traces from the Agilent Tape station, total number of reads (> 27 million unique reads aligned), peak at 150 bp and normal distribution, and mean target coverage of 1,534 reads.

On initial review of somatic variants (which were not germline variants), the mutational spectrum of the tumor was consistent with known patterns for colorectal cancer, including inactivating mutations in *APC* and an activating mutation in *PIK3CA*.⁵ An inactivating mutation was also noted in *MLH1*, a gene associated with a subset of colon cancers demonstrating the microsatellite instability high (MSI-H) phenotype. Supporting the

MSI-H phenotype was the large number of mutations observed in the tumor sample, with an estimated mutation rate of more than 200 mutations per megabase of captured sequence (> 1,000 mutations in the approximately 5 MB of targeted sequence). Select protein-coding mutations in genes previously associated with colon cancer are listed in [Table 1](#).

Review of the mutant allele fractions of *APC* and *PIK3CA* was potentially informative as to the nature of the tumor genome. Fifty-three percent of the bases detected at position 1489 of *APC* contained the inactivating allele. By contrast, only 28% of the bases of *PIK3CA* at position 1047 had the activating allele. An additional two mutations in *APC* were observed to have approximately 25% mutant allele frequency. One interpretation of the data is that the specimen consisted of nearly 100% tumor nuclei in a genome that was tetraploid. In such a case, there might have been an initial *APC*

Fig 2. (A) Low- and (B) high-resolution images of tumor biopsy sample with hematoxylin and eosin stain. Tumor is a moderately differentiated adenocarcinoma and demonstrates mixed inflammatory infiltrate. Percentage of tumor nuclei was estimated at 60%.

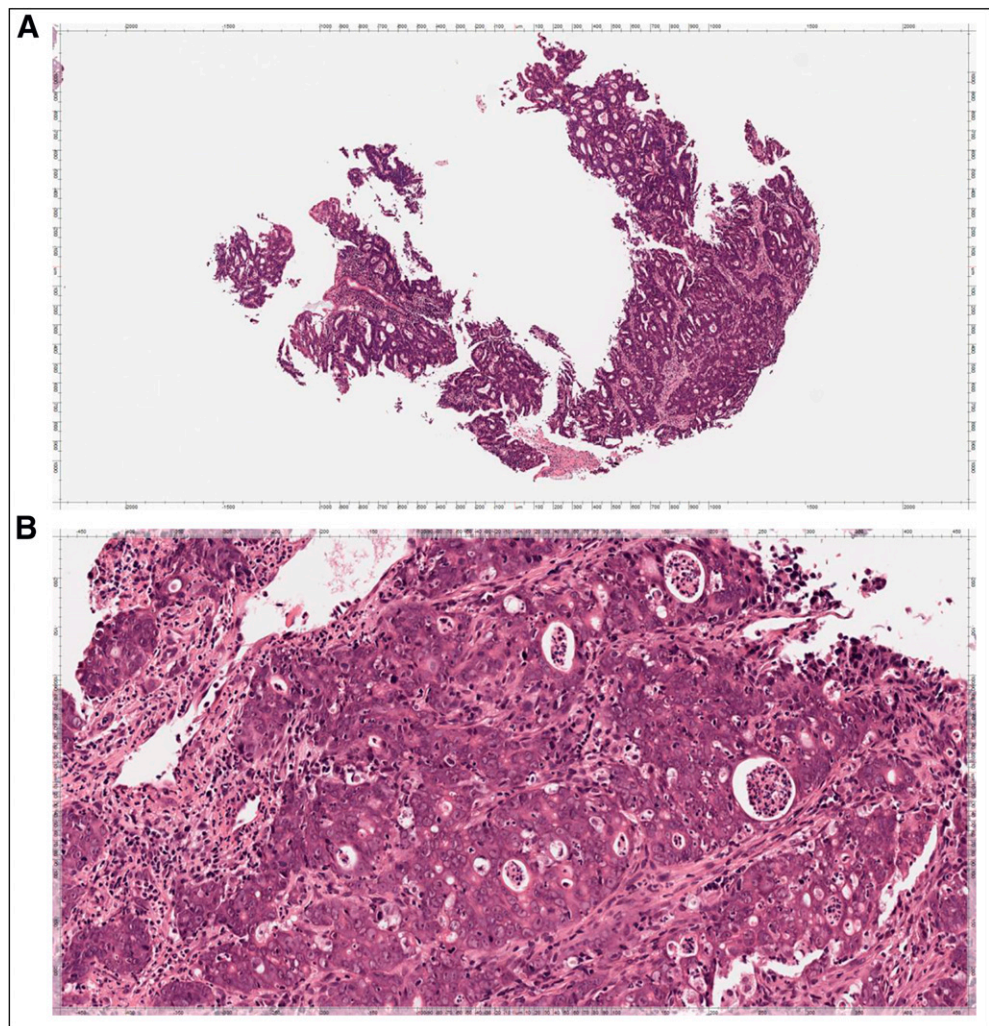


Table 1. Select Protein-Coding Mutations in Patient's Primary Tumor by Whole-Genome Sequencing

Gene	Chromosome	Coordinate	cDNA	Protein	Effect	MAF (%)	Q	COSMIC ⁶
<i>MLH1</i>	3	37089122	c.1852_1854delAAG	p.Lys618del	Codon deletion	54	366	3
<i>TGFBR2</i>	3	30691871	c.383delA	p.Lys128fs	Frameshift	54	NA*	5
<i>APC</i>	5	112175755	c.4464_4465insT	p.Leu1489fs	Frameshift	53	517	44
<i>NRAS</i>	1	115252312	c.328C>T	p.Pro110ser	Nonsynonymous coding	33	436	0
<i>PIK3CA</i>	3	178952085	c.3140A>G	p.His1047Arg	Nonsynonymous coding	28	346	1,906
<i>APC</i>	5	112170693	c.1789G>A	p.Ala597Thr	Nonsynonymous coding	28	380	1
<i>APC</i>	5	112179035	c.7748delA	p.Ala2584fs	Frameshift	25	376	1
<i>ARID1A</i>	1	27100175	c.3977delC	p.Pro1326fs	Frameshift	21	284	1
<i>TOP1</i>	20	39657712	c.5G>A	p.Ser2Asn	Nonsynonymous coding	15	45	0
<i>TOP1</i>	20	39721171	c.674C>T	p.Pro225Leu	Nonsynonymous coding	10	491	0

NOTE. Protein-coding mutations selected from 1,192 somatic mutations identified; organized top to bottom by MAF.

Abbreviations: COSMIC, Catalogue of Somatic Mutations in Cancer; MAF, mean allelic frequency; NA, not applicable; Q, $-10 \times \log_{10}$ (probability of sequencing error).

*Q score not defined for this deletion event.

mutation in 1489 followed by genome doubling, resulting in two mutant alleles and two wild-type alleles. This event was followed by independent separate mutations, resulting in 25% mutant allele fractions and complete loss of functional *APC*. The mutation in *PIK3CA*, as well as most of the more than 1,000 mutations, occurred after genome doubling, because the most common mutant allele fractions were approximately 25%. Tumor evolution in this manner suggests a mechanism by which a cell with so many mutations might remain viable by offering four alleles to retain at least one functional form of the gene.

Despite the large number of mutations, the cancer genome remained structurally intact (Fig 3). Genomes without such copy-number changes are uncommon, with nearly every colon cancer demonstrating amplifications or deletions.⁷ The only evidence of genome instability in this patient case involved low-level gains of chromosomes 17 and 19 and perhaps loss of a portion of chromosome 13. If the supposition of a tetraploid genome is correct, these events might best be explained by loss or gain of an additional chromosome from an average copy of four alleles. Interestingly, it has been suggested that tumors that retain wild-type *TP53* and/or are of the MSI-H phenotype are more likely to have a stable genome configuration, such as we saw in our patient case.^{8,9} In our patient case, despite the large number of mutations, no evidence for *TP53* mutation was detected. This is also consistent with the observation that the frequency of *TP53* mutations is lower in MSI-H tumors.¹⁰

Although the MSI-H phenotype with hypermutation in association with *MLH1* alteration is an

established entity,¹⁰ the overall number of mutations in this patient case was particularly striking, leading us to ask whether any additional alterations might play a role. Specifically, we queried whether previously reported mutations in *POLE* might be present.⁸ Because *POLE* was not included in the original hybrid capture set, the remaining DNA was submitted for whole-exome sequencing, and no *POLE* mutation was detected. Next, we considered the possibility of a somatic mutation in another gene in the same family, *POLD1*, because germline mutations in *POLD1* have been described as drivers of colorectal cancer.^{11,12} Interrogation of the *POLD1* sequence revealed a somatic c.2171G>A [p.Gly724Glu] mutation (Fig 4) that was subsequently validated by Sanger sequencing. This particular mutation has not previously been reported as a driver mutation in colorectal cancer, but it is in close proximity to a cluster of previously reported mutations in the DNA polymerase B domain.^{11,12}

Analysis of TCGA Data

To put the findings from our patient case into the context of prior reports in colorectal cancer, we turned to TCGA.⁸ TCGA confirmed the presence of somatic *POLE* mutations in 31 patient cases (7.2%). *POLD1* mutations were observed in 17 patient cases (4.0%), just below the 5% rate targeted for detection in TCGA. Five cancers (1.2%) contained both *POLE* and *POLD1* mutations. When examining the distribution of non-silent somatic mutations in *POLE*, we observed that they were spread across all coding domains of the gene; however, mutations in the DNA polymerase B exonuclease domain were strongly

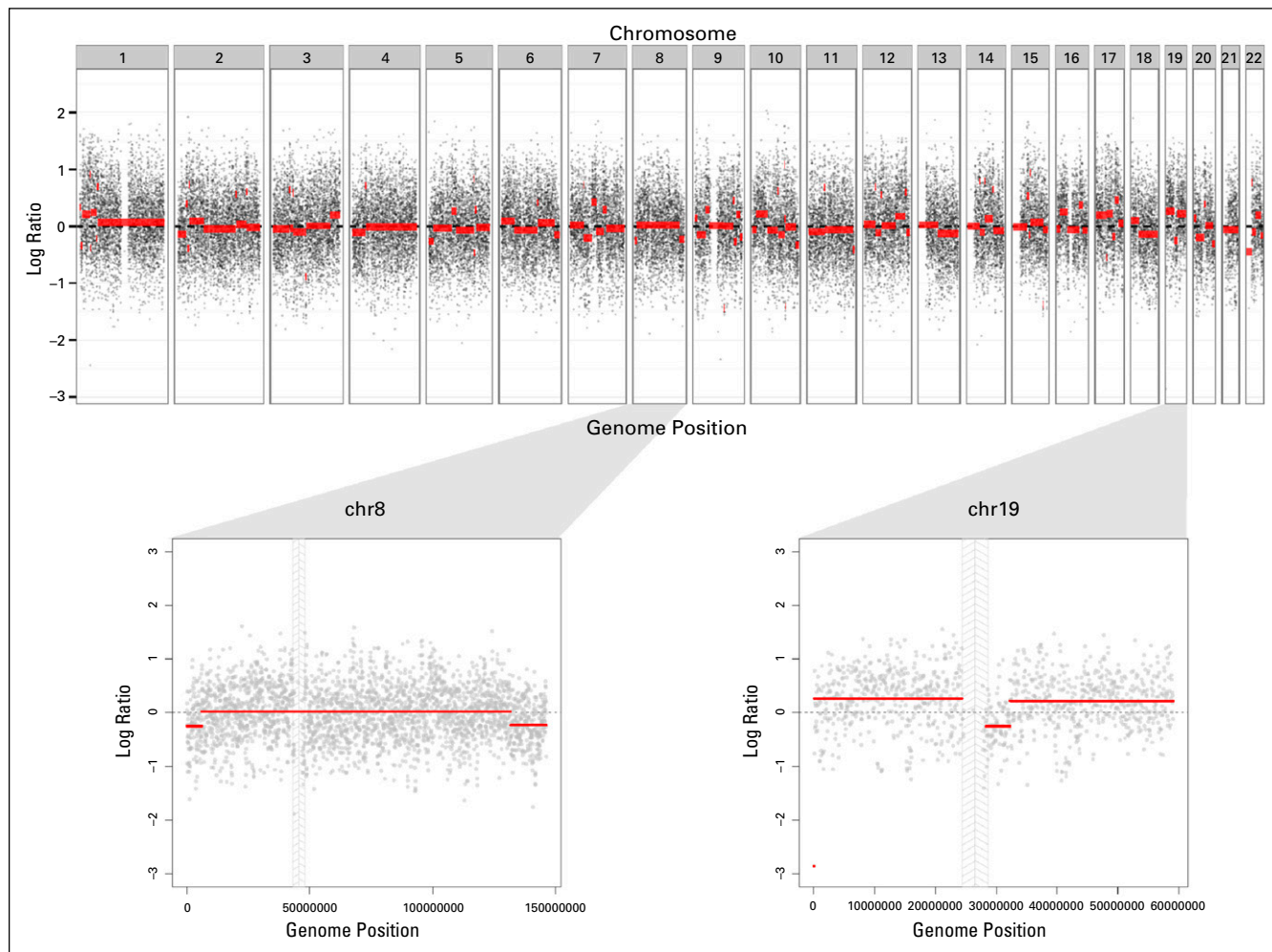


Fig 3. Copy-number variations (CNVs) from genome-wide sequencing results from the primary tumor of this patient. Red lines are fitted CNV numbers obtained from sequenced variants (dots on the plot). Chromosome 8 (chr8) and chr19 are magnified to illustrate no significant CNVs (chr8) and low-level gains (chr19).

associated with ultra-high mutation rates ($> 2,000$ mutations; Fig 4, top). Nonsilent somatic mutations in *POLD1* were located mainly in the exonuclease and polymerase B domains (Fig 4, bottom). We then looked for associations of *POLE* and *POLD1* mutations with both overall mutation rate and the pattern of hyper-indel hypermutation seen in our patient case (Fig 5A). This inquiry revealed a divergence in patterns between *POLE* and *POLD1* mutations. Colorectal cancers with ultra-high mutation rates ($> 2,000$ nonsilent somatic mutations) invariably exhibited mutations in *POLE*, but not all *POLE* mutations were associated with ultra-high mutation rates. Strikingly, however, the fraction of indels among all mutations in these patient cases remained low, generally below 5%. By contrast, cancers with *POLD1* mutations were not associated with ultra-high mutation rates, although the median number of nonsilent mutations was much higher (893 mutations) than the median for the entire data set (134 mutations). Consistent with our report, *POLD1* mutants were associated with a high rate of indels

(17% of all mutations). All *POLD1* mutations occurred in the set of tumors described as MSI-H. By contrast, there were 52 MSI-H tumors that did not have *POLD1* mutations. Cancers with *POLE* and/or *POLD1* mutations generally were hypermutated, with only seven patient cases (1.6%) having fewer than 200 nonsilent somatic mutations.

We considered the possibility that, because the set of samples being considered included those with the highest mutation rates, mutations of *POLD1* might simply occur by random chance. The probability of detecting 15 *POLD1* mutations in these samples was < 0.001 (Fisher's exact test). Further arguing against chance alone, we noted that *POLD1* mutations were not observed in any of the patient cases of *POLE* ultramutated tumors but rather uniquely in patients with MSI-H phenotype with high numbers of indels. Finally, the clustering of mutations within the DNA polymerase B domain of the gene supports the hypothesis that these are not random mutations.

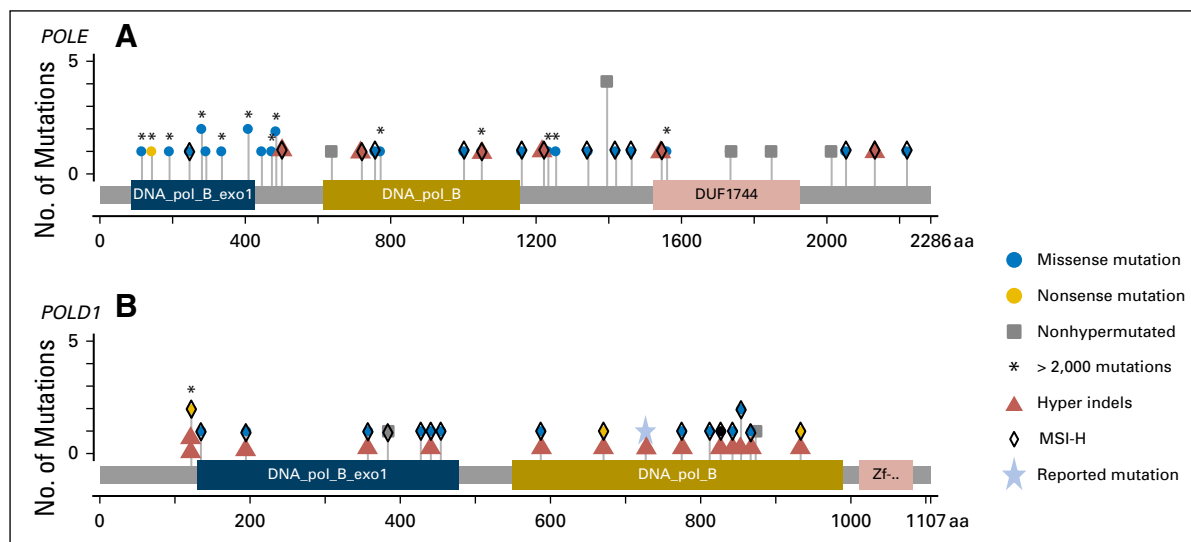


Fig 4. Lollipop plots showing mutations in (A) *POLE* and (B) *POLD1* from The Cancer Genome Atlas (TCGA), as well as (B) the mutation in *POLD1* from our patient. Somatic mutations identified in the colorectal TCGA data set were broadcast onto the gene model as provided by cBioPortal (<http://www.cbioportal.org>). This gene model includes important functional domains of the gene: DNA_pol_B_exo1, DNA polymerase beta exonuclease 1 domain; DNA_pol_B, DNA polymerase, family B domain; DUF1744, domain of unknown function found on epsilon catalytic subunit of DNA polymerase; zf..., zf-C4pol (C4-type zinc-finger of DNA polymerase delta). All domains were annotated from the Pfam database. MSI-H, microsatellite instability high.

Because *POLD1* mutations were associated with MSI-H phenotype, we considered the possibility that these mutations were a passenger event confined to the biology of MSI-H cancers. Comparison of indel rate in MSI-H cancers on the basis of *POLD1* mutation status revealed that MSI-H cancers with *POLD1* mutations exhibited approximately 60% more indels than MSI-H cancers without *POLD1* mutations ($P < .03$; Fig 5B). Not surprisingly, hypermutated cancers exhibited a much higher indel rate than nonhypermutated cancers ($P < .001$; Fig 5C). However, *POLE*-hypermutated cancers exhibited approximately 50% fewer indels than hypermutated cancers without *POLE* mutations ($P < .001$; Fig 5C).

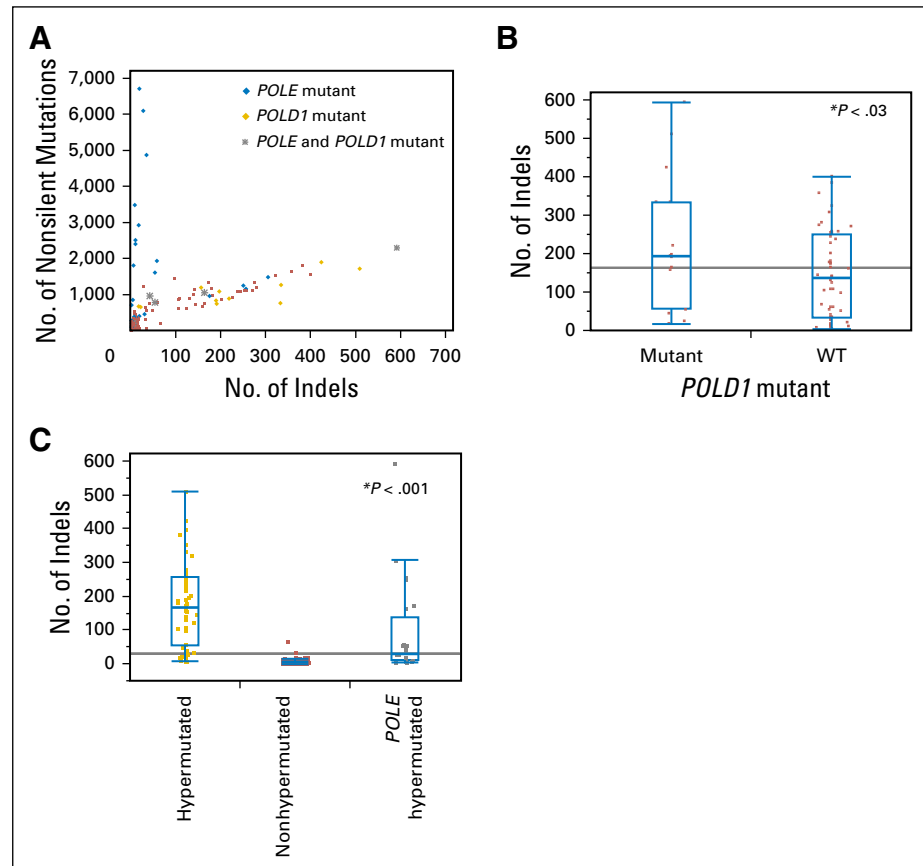
DISCUSSION

CRs to chemotherapy have been described previously in patients with colorectal cancer. A recent meta-analysis of chemotherapy plus bevacizumab reported a CR rate of 2.4% based on aggregate data from seven randomized controlled trials.¹³ Because these responses are infrequent, and many of them occurred in the era before genomic profiling of tumors, the links between tumor genomics and exceptional responses are unclear. Having observed a CR to FOLFIRI and bevacizumab that has been durable for 5 years in the patient case presented here, sequencing of tumor and germline DNA was undertaken to search for alterations associated with this exceptional response. A similar strategy is being used in the exceptional responders' protocol sponsored by the National Cancer Institute (ClinicalTrials.gov identifier NCT02243592). TCGA Network reported on the molecular characterization of human colon and rectal cancers in

2012.⁶ Tumors were classified as nonhypermutated versus hypermutated, with the latter having mutations in more than 12×10^6 bases and a median of 728 mutations on exome sequencing. Hypermutated tumors were more likely to originate in the right colon and could be further classified into two types: a majority with MSI-H that had relatively fewer mutations, and a minority without MSI-H that had relatively more mutations (ultramutated). MSI-H tumors typically had hypermethylation and *MLH1* silencing, whereas hypermutated tumors without MSI-H typically had somatic mutations in one or more mismatch-repair genes and/or *POLE*. Right-sided colon cancers were recently reported to be associated with worse prognosis compared with left-sided colon cancers in a systematic review and meta-analysis,¹⁴ but it is not clear whether the same would be true for hypermutated right-sided colon cancers.

DNA polymerases ϵ (*POLE*) and δ (*POLD1*) are the two main enzymes involved in human DNA replication. Germline and somatic mutations in the exonuclease (proofreading) domains of *POLE* and *POLD1* are associated with ultramutated colorectal and endometrial cancers.^{12,15} Whole-genome sequencing in our patient case showed a hypermutated (but not ultramutated) phenotype in this right-sided tumor with many indels including a codon deletion of *MLH1*, so the decision was made to pursue whole-exome sequencing to search for additional mutations in *POLE* or *POLD1*. We identified and validated a *POLD1* mutation in this patient's tumor. Importantly, this mutation was not in the exonuclease domain but was located in a functional domain.

Fig 5. (A) Nonsilent mutations versus insertions or deletions (indels) for *POLE*- and *POLD1*-mutant tumors from The Cancer Genome Atlas (TCGA). Numbers of nonsilent mutations and indels were calculated for each colorectal tumor from the TCGA data set (n = 430). Tumors with somatic mutations in *POLE* (blue), *POLD1* (gold), or both *POLE* and *POLD1* (gray) are distinguished from tumors without *POLE* or *POLD1* mutations (red). (B) Indels in *POLD1*-mutant versus wild-type (WT) tumors with microsatellite instability high (MSI-H) phenotype from TCGA. Number of indel was calculated for the 67 MSI-H tumors from the colorectal TCGA data set. MSI-H tumors that also had *POLD1* somatic mutations exhibited more indels as compared with MSI-H tumors without *POLD1* somatic mutations (mean *POLD1*-mutant indels, n = 230; mean *POLD1* WT indels, n = 144). (C) Indels among hypermutated (n = 50), nonhypermutated (n = 356), and *POLE*-hypermutated (n = 24) tumors from TCGA (total, n = 430; mean hypermutated indels, n = 176; mean nonhypermutated indels, n = 6; mean *POLE*-hypermutated indels, n = 91). (*) Two-sided *t* test.



Analysis of TCGA confirmed that the observed phenotype was similar to other tumors with *POLD1* mutations. We found that *POLD1*-mutated tumors have relatively greater numbers of indels than *POLD1* wild-type tumors, including those with *POLE* mutations. To our knowledge, this is a pattern that has not previously been reported in the literature.

Two previous studies have attempted to relate *POLE* mutations to colorectal cancer outcomes. In a population-based cohort with microsatellite-stable stage I to IV colorectal cancer, Stenzinger et al¹⁶ reported a trend toward shorter survival for patients with *POLE* mutations compared with their counterparts without *POLE* mutations. Along the same lines, there was a statistically significantly increased mortality for patients with stage III to IV colorectal cancer receiving chemotherapy with *POLE* mutations compared with their counterparts without *POLE* mutations.¹⁶ In contrast, Domingo et al¹⁷ recently reported that *POLE* mutations were associated with a lower risk of recurrence compared with microsatellite-stable stage II to III colorectal cancers, with correlative data suggesting that these tumors were more immunogenic. Rizvi et al¹⁸ showed that

higher nonsynonymous mutation burden was associated with markers of immunogenicity and improved outcomes with programmed death-1 blockade in non-small-cell lung cancer. In our analyses of data from TCGA, there were no statistically significant differences in survival based on overall mutation status, *POLE* mutation status, *POLD1* mutation status, or combined *POLE* and *POLD1* mutation status (Appendix Fig A1).

An important limitation of this study is that it was impossible to isolate the genomic alterations most important in this patient's exceptional response. It is reasonable to postulate that the *POLD1* mutation led to the somatic codon deletion of *MLH1* and the MSI-H phenotype. Analysis of CALGB 89803 suggested that patients with MSI-H colon cancer had improved disease-free survival in a study of FU plus leucovorin versus FOLFIRI as adjuvant therapy for stage II to III disease.¹⁹ If the mutations in topoisomerase I (*TOP1*) are gain-of-function mutations and/or result in gene amplification (their function is unknown), this might increase sensitivity to irinotecan (a topoisomerase I-interacting drug), because higher copy numbers of this gene have been linked to irinotecan sensitivity in vitro.²⁰ Finally, given the link between

mutation burden and immunogenicity,¹⁸ it is also possible that chemotherapy induced an endogenous immune response to a variety of neoantigens in this patient's cancer.

In conclusion, an exceptional response in a patient with metastatic colorectal cancer to FOLFIRI plus bevacizumab led us to identify a somatic mutation in *POLD1*. In TCGA, *POLD1* mutants have a hypermutated phenotype with a

large number of indels compared with their wild-type and *POLE*-mutant counterparts. This study is hypothesis generating and supports the sequencing of *POLE* and *POLD1* in patients with exceptional responses to better understand the potential link between tumor genomics and response to chemotherapy.

DOI: [10.1200/PO.16.00015](https://doi.org/10.1200/PO.16.00015)

Published online on ascopubs.org/journal/po on April 27, 2017.

AUTHOR CONTRIBUTIONS

Conception and design: Manish R. Sharma, Elena Marangon, Giuseppe Toffoli, D. Neil Hayes, Federico Innocenti

Financial support: D. Neil Hayes

Administrative support: Stergios J. Moschos, D. Neil Hayes

Provision of study materials or patients: D. Neil Hayes

Collection and assembly of data: Manish R. Sharma, James T. Auman, Nirali M. Patel, Juneko E. Grilley-Olson, Stergios J. Moschos, Xiaoying Yin, Michele C. Hayward, Blase N. Polite, Bianca Posocco, Giuseppe Toffoli, D. Neil Hayes, Federico Innocenti

Data analysis and interpretation: Manish R. Sharma, James T. Auman, Nirali M. Patel, Xiaobei Zhao, Stergios J. Moschos, Joel S. Parker, Blase N. Polite, Elena Marangon, Bianca Posocco, D. Neil Hayes, Federico Innocenti

Manuscript writing: All authors

Final approval of manuscript: All authors

Accountable for all aspects of the work: All authors

AUTHORS' DISCLOSURES OF POTENTIAL CONFLICTS OF INTEREST

Exceptional Chemotherapy Response in Metastatic Colorectal Cancer Associated With Hyper-Indel-Hypermutated Cancer Genome and Comutation of *POLD1* and *MLH1*

The following represents disclosure information provided by authors of this manuscript. All relationships are considered compensated. Relationships are self-held unless noted. I = Immediate Family Member, Inst = My Institution. Relationships may not relate to the subject matter of this manuscript. For more information about ASCO's conflict of interest policy, please refer to www.asco.org/rwc or po.ascopubs.org/site/ifc.

Manish R. Sharma

Consulting or Advisory Role: EMD Serono, Ipsen, Bayer

James T. Auman

No relationship to disclose

Nirali M. Patel

No relationship to disclose

Juneko E. Grilley-Olson

Consulting or Advisory Role: Sanofi

Research Funding: Bayer, Novartis (Inst), Peregrine Pharmaceuticals (Inst), NanoCarrier (Inst), Genentech (Inst), Seattle Genetics (Inst), MedImmune (Inst), GlaxoSmithKline (Inst), Pfizer (Inst)

Xiaobei Zhao

No relationship to disclose

Stergios J. Moschos

Consulting or Advisory Role: Merck Sharp & Dohme, Amgen, Paometheus, Castle Biosciences

Research Funding: Merck Sharp & Dohme, Pharmacyclics, Amgen, Genentech/Roche

Travel, Accommodations, Expenses: Bristol-Myers Squibb, Merck Sharp & Dohme, Novartis

Joel S. Parker

No relationship to disclose

Xiaoying Yin

No relationship to disclose

Michele C. Hayward

No relationship to disclose

Blase N. Polite

Consulting or Advisory Role: AstraZeneca, Pfizer

Speakers' Bureau: Bayer/Onyx

Research Funding: Merck

Other Relationship: Gerson Lehrman Group

Elena Marangon

No relationship to disclose

Bianca Posocco

No relationship to disclose

Giuseppe Toffoli

No relationship to disclose

D. Neil Hayes

Leadership: GeneCentric

Stock and Other Ownership Interests: GeneCentric

Consulting or Advisory Role: GeneCentric

Patents, Royalties, Other Intellectual Property: I hold several diagnostic patents or pending patents in the area of solid tumor diagnostics

Federico Innocenti

Patents, Royalties, Other Intellectual Property: Royalties from the Mayo Foundation on the UGT1A1 testing

ACKNOWLEDGMENT

We thank the patient for her enthusiasm in participating in the clinical trial and subsequent correlative studies. We also thank Mark Ratain, MD, and Yusuke Nakamura, MD, for their valuable discussions regarding this patient case.

Affiliations

Manish R. Sharma and **Blase N. Polite**, University of Chicago Medicine, Chicago, IL; **James T. Auman**, **Nirali M. Patel**, **Juneko E. Grilley-Olson**, **Xiaobei Zhao**, **Stergios J. Moschos**, **Joel S. Parker**, **Xiaoying Yin**, **Michele C. Hayward**, **D. Neil Hayes**, and **Federico Innocenti**, University of North Carolina at Chapel Hill, Chapel Hill, NC; and **Elena Marangon**, **Bianca Posocco**, and **Guisepppe Toffoli**, Centro di Riferimento Oncologico, Aviano, Italy.

Support

Supported by National Cancer Institute Award No. K12CA139160 (M.R.S.), National Institutes of Health Award No. U10CA181009 (D.N.H.), funds from the University of North Carolina Lineberger Comprehensive Cancer Center and Eshelman School of Pharmacy (F.I.), and Italian Association for Cancer Research Project No. IG 10325.

REFERENCES

1. Toffoli G, Sharma MR, Marangon E, et al: Genotype-guided dosing study of FOLFIRI plus bevacizumab in metastatic colorectal cancer patients. *Clin Cancer Res* 23:918-924, 2017
2. Therasse P, Arbuck SG, Eisenhauer EA, et al: New guidelines to evaluate the response to treatment in solid tumors: European Organisation for Research and Treatment of Cancer, National Cancer Institute of the United States, National Cancer Institute of Canada. *J Natl Cancer Inst* 92:205-216, 2000
3. Zhao X, Wang A, Walter V, et al: Combined targeted DNA sequencing in non-small cell lung cancer (NSCLC) using UNCseq and NGScopy, and RNA sequencing using UNCqer for the detection of genetic aberrations in NSCLC. *PLoS One* 10:e0129280, 2015
4. The Cancer Genome Atlas: TCGA data portal. <https://tcga-data.nci.nih.gov/docs/publications/tcga/>
5. Day FL, Jorissen RN, Lipton L, et al: PIK3CA and PTEN gene and exon mutation-specific clinicopathologic and molecular associations in colorectal cancer. *Clin Cancer Res* 19:3285-3296, 2013
6. COSMIC: Catalogue of Somatic Mutations in Cancer. <http://cancer.sanger.ac.uk/cosmic>
7. Sheffer M, Bacolod MD, Zuk O, et al: Association of survival and disease progression with chromosomal instability: A genomic exploration of colorectal cancer. *Proc Natl Acad Sci USA* 106:7131-7136, 2009
8. Cancer Genome Atlas Network: Comprehensive molecular characterization of human colon and rectal cancer. *Nature* 487:330-337, 2012
9. Westra JL, Boven LG, van der Vlies P, et al: A substantial proportion of microsatellite-unstable colon tumors carry TP53 mutations while not showing chromosomal instability. *Genes Chromosomes Cancer* 43:194-201, 2005
10. Lin EI, Tseng LH, Gocke CD, et al: Mutational profiling of colorectal cancers with microsatellite instability. *Oncotarget* 6:42334-42344, 2015
11. Mertz TM, Sharma S, Chabes A, et al: Colon cancer-associated mutator DNA polymerase δ variant causes expansion of dNTP pools increasing its own infidelity. *Proc Natl Acad Sci USA* 112:E2467-E2476, 2015
12. Briggs S, Tomlinson I: Germline and somatic polymerase ϵ and δ mutations define a new class of hypermutated colorectal and endometrial cancers. *J Pathol* 230:148-153, 2013
13. Zhang G, Zhou X, Lin C: Efficacy of chemotherapy plus bevacizumab as first-line therapy in patients with metastatic colorectal cancer: A meta-analysis and up-date. *Int J Clin Exp Med* 8:1434-1445, 2015
14. Petrelli F, Tomasello G, Borgonovo K, et al: Prognostic survival associated with left-sided vs right-sided colon cancer: A systematic review and meta-analysis. *JAMA Oncol* [epub ahead of print on October 27, 2016]
15. Palles C, Cazier JB, Howarth KM, et al: Germline mutations affecting the proofreading domains of POLE and POLD1 predispose to colorectal adenomas and carcinomas. *Nat Genet* 45:136-144, 2013
16. Stenzinger A, Pfarr N, Endris V, et al: Mutations in POLE and survival of colorectal cancer patients: Link to disease stage and treatment. *Cancer Med* 3:1527-1538, 2014
17. Domingo E, Freeman-Mills L, Rayner E, et al: Somatic POLE proofreading domain mutation, immune response, and prognosis in colorectal cancer: A retrospective, pooled biomarker study. *Lancet Gastroenterol Hepatol* 1:207-216, 2016
18. Rizvi NA, Hellmann MD, Snyder A, et al: Cancer immunology: Mutational landscape determines sensitivity to PD-1 blockade in non-small cell lung cancer. *Science* 348:124-128, 2015
19. Bertagnolli MM, Redston M, Compton CC, et al: Microsatellite instability and loss of heterozygosity at chromosomal location 18q: Prospective evaluation of biomarkers for stages II and III colon cancer—A study of CALGB 9581 and 89803. *J Clin Oncol* 29:3153-3162, 2011
20. Rømer MU, Jensen NF, Nielsen SL, et al: TOP1 gene copy numbers in colorectal cancer samples and cell lines and their association to in vitro drug sensitivity. *Scand J Gastroenterol* 47:68-79, 2012

APPENDIX

Table A1. Demographic and Clinical Characteristics of Patient Cases in Analyses From TCGA Colon and Rectal Adenocarcinoma Cohorts

Characteristic	No. (%)
Anatomic site	
Colon	330 (77)
Rectum	99 (23)
Not available	1
Age, years	
31-45	25 (6)
46-60	92 (21)
61-75	198 (46)
≥ 75	115 (27)
Sex	
Female	194 (45)
Male	236 (55)
Race	
American Indian or Alaskan Native	1
Asian	11 (3)
Black	21 (5)
White	214 (50)
Not available	183 (43)
Pathologic stage	
I	82 (19)
II	155 (36)
III	121 (28)
IV	61 (14)
Not available	11 (3)
Total	430

Abbreviation: TCGA, The Cancer Genome Atlas.

Fig A1. Kaplan-Meier survival curves for cases of colorectal cancer from The Cancer Genome Atlas with survival and somatic mutation data. Survival curves were generated on different data subsets based on (A) hypermutation status (hypermutated, n = 78 [deaths, n = 12]; nonhypermutated, n = 305 [deaths, n = 70]; log-rank $\chi^2 = 0.5020$; Wilcoxon $\chi^2 = 0.7898$), (B) *POLE* mutations (*POLE* mutated, n = 32 [deaths, n = 5]; wild type [WT], n = 450 [deaths, n = 78]; log-rank $\chi^2 = 0.626$; Wilcoxon $\chi^2 = 0.8993$), (C) *POLD1* mutations (*POLD1* mutated, n = 17 [deaths, n = 6]; WT, n = 465 [deaths, n = 77]; log-rank $\chi^2 = 0.0322$; Wilcoxon $\chi^2 = 0.1052$), or (D) combined *POLE* and *POLD1* mutations (*POLE* and *POLD1* mutated, n = 44 [deaths, n = 8]; WT, n = 438 [deaths, n = 75]; log-rank $\chi^2 = 0.9852$; Wilcoxon $\chi^2 = 0.7380$). For all analyses, survival was capped at 60 months.

